Received: 30 November 2019 | Revised: 1 February 2020 | Accepted: 10 February 2020

DOI: 10.1002/mbo3.1017

ORIGINAL ARTICLE

MicrobiologyOpen Open Access WILEY

Detection of methicillin-resistant *Staphylococcus aureus* persistence in osteoblasts using imaging flow cytometry

Dafne Bongiorno[1] | **Nicolò Musso**[2] | **Lorenzo Mattia Lazzaro**[1] | **Gino Mongelli**[1] | **Stefania Stefani**[1,2] | **Floriana Campanile**[1]

[1]Department of Biomedical and Biotechnological Sciences (BIOMETEC), Medical Molecular Microbiology and Antibiotic Resistance Laboratory (MMAR*Lab*), University of Catania, Catania, Italy

[2]Bio-nanotech Research and Innovation Tower (BRIT), University of Catania, Catania, Italy

Correspondence
Dafne Bongiorno, Department of Biomedical and Biotechnological Sciences (MMARL), University of Catania, Via Santa Sofia, 97, 95123 Catania, Italy.
Email: d.bongiorno@unict.it

Abstract

Methicillin-resistant *S. aureus* has been reported as the main pathogen involved in chronic infections, osteomyelitis, and prosthetic joint infections. The host/pathogen interaction is dynamic and requires several changes to promote bacterial survival. Here, we focused on the internalization and persistence behavior of well-characterized *Staphylococcus aureus* invasive strains belonging to the main ST-MRSA-SCC*mec* clones. To overcome the limitations of the cell culture method, we comparatively analyzed the ability of internalization within human MG-63 osteoblasts with imaging flow cytometry (IFC). After evaluation by cell culture assay, the MRSA clones in the study were all able to readily internalize at 3h postinfection, the persistence of intracellular bacteria was evaluated at 24h both by routine cell culture and IFC assay, after vancomycin-BODIPY staining. A statistical difference of persistence was found in ST5-SCC*mec*II (26.59%), ST228-SCC*mec*I (20.25%), ST8-SCC*mec*IV (19.52%), ST239-SCC*mec*III (47.82%), and ST22-SCC*mec*IVh (50.55%) showing the same ability to internalize as ATCC12598 (51%), the invasive isolate used as control strain for invasion and persistence assays. We demonstrated that the intracellular persistence process depends on the total number of infected cells. Comparing our data obtained by IFC with those of the cell culture assay, we obtained greater reproducibility rates and a number of intracellular bacteria, with the advantage of analyzing live host cells. Moreover, with some limitations related to the lack of whole-genome sequencing analysis, we validated the different proclivities to persist in the main Italian HA-MRSA invasive isolates and our results highlighted the heterogeneity of the different clones to persist during cell infection.

KEYWORDS

genetic background, imaging flow cytometry, internalization, methicillin-resistant *S. aureus*, osteoblast

Bongiorno and Musso equally contributed to this work.

This is an open access article under the terms of the Creative Commons Attribution-NonCommercial-NoDerivs License, which permits use and distribution in any medium, provided the original work is properly cited, the use is non-commercial and no modifications or adaptations are made.
© 2020 The Authors. *MicrobiologyOpen* published by John Wiley & Sons Ltd.

1 | INTRODUCTION

Staphylococcus aureus is one of the most adaptable human pathogens and is able to infect many organs and damage tissues, causing severe infections. One of the most interesting strategies is associated with its persistence, through changes from the aggressive wild-type phenotype to small colony variant (SCV) forms, more adaptive long-term persistent cells. In these dynamic changes, it becomes refractory to prolonged antimicrobial treatment required for chronic infections, recurrent osteomyelitis (OM), and prosthetic joint infections (PJIs); Tuchscherr & Löffler, 2016). In particular, PJIs can have a dramatic impact on the quality of life of a patient, often requiring surgical intervention and prosthesis removal (Moore et al., 2017; Purrello et al., 2016; Stefani et al., 2012).

Even if the prevalence of methicillin-resistant *S. aureus* (MRSA) in these infections is lower than that of MSSA, these human pathogens are still problematic because they are often associated with antimicrobial resistance, leading to high rates of hospitalization and mortality as well as the burden of associated costs (Gould et al., 2011).

In the assessment of the interaction between *S. aureus* isolates and osteoblasts during PJIs and OM, three events are crucial: adhesion, invasion, and the postinvasion process or internalization. Adhesion of *S. aureus* to host structures is a prerequisite for colonization and disease development and relies on the expression of a large number of cell surface proteins (adhesins) of the microbial surface component recognizing adhesive matrix molecules (MSCRAMM) and of the secretable expanded repertoire adhesive molecules (SERAM) classes. *S. aureus* osteoblast invasion plays a crucial role in the initiation and maintenance of inflammatory immune responses (Sinha & Fraunholz, 2010). Recent studies have demonstrated that *S. aureus* is able to internalize in the osteoblast cytoplasm, and this localization can represent a reservoir of bacteria for chronic disease (Horn, Stelzner, Rudel, & Fraunholz, 2018).

During postinvasion events, *S. aureus* is internalized in osteoblasts via a process that involves actin microfilaments, microtubules, receptor-mediated endocytosis, and activation of signal transduction cascades. Osteoblasts release viable staphylococci, which are then able to reinfect and internalize in new osteoblasts, representing the potential key for prolonged and persistent infections (Garzoni & Kelley, 2009; Josse, Velard, & Gangloff, 2015). Many papers have reported *S. aureus* internalization in osteoblasts considering diverse aspects related to the mechanism of pathogenicity (Jevon et al., 1999), the induction of various responses from the osteoblasts (Josse et al., 2016), and their impact on the interaction between osteoclasts and osteoblasts (Josse et al., 2015).

Furthermore, different cell culture models have been used to study the frequency of internalization of *Staphylococcus* spp. in osteoblasts. These assays involve the use of gentamicin or lysostaphin to eliminate the external and adherent bacterial cells, and the quantification of live bacteria is performed by host cell lysis and plate counting (Jevon et al., 1999; Valour et al., 2013; Wright & Friedland, 2004). As reported in many papers, this method is time-consuming and lacks reproducibility (Trouillet et al., 2011).

Taking into consideration the disadvantages of the cell culture gold standard assay and the heterogeneity of the main Italian *S. aureus* invasive isolates recently described in 2015 (Campanile et al., 2015), we aimed to (a) provide a novel method of detection of intracellular *S. aureus* by analyzing live host cells through imaging flow cytometry (IFC) to strengthen the conventional cell culture method and (b) confirm the reliability and reproducibility of this method validating the different proclivities to persist during cell infection (at 24 hr p.i.) of the main HA-MRSA invasive isolates responsible for bone infections and PJIs, belonging to different epidemic clones.

2 | MATERIAL AND METHODS

2.1 | Strains included in the study

The study sample consisted of 15 invasive MRSA isolates already molecularly characterized by standard genotyping methods internationally recognized as defining MRSA clones, and belonging to ST239-SCC*mec*III, ST5-SCC*mec*II, ST8-SCC*mec*IV, ST228-SCC*mec*I, and ST22-SCC*mec*IVh, three strains for each clone. These strains were selected from a large collection of 640 MRSA strains isolated during an Italian national survey that was carried out in 2012. All the strains were phenotypically and molecularly characterized (Table A1) as previously reported (Bongiorno, Mongelli, Stefani, & Campanile, 2018; Campanile et al., 2015). The invasive isolate ATCC12598 (Cowan ST30-t076; ATCC® Standards Development Organization, LGC Standards S.r.l.) was used as control strain for invasion and persistence assays and for the statistical analysis of the results obtained with the cell culture method and IFC (McPherson et al., 2008).

2.2 | Eukaryotic cell culture preparation

Infection experiments were performed on the human osteosarcoma cell line MG-63 (ATCC® CRL-1427™; Standards Development Organization, LGC Standards S.r.l.). During the expansion period, the cells were grown in 75 cm^2 flasks with modified Eagle's medium (MEM), HEPES, GlutaMAX™ Supplement (cat. No. 42360024, containing 1 g/L D-glucose, GIBCO™; Thermo Fisher Scientific Monza, Italy), supplemented with 10% FBS (fetal bovine serum; cat. No. 16000044, GIBCO™; Thermo Fisher Scientific) and 100 U/ml of penicillin/streptomycin (cat. No. 15070063 GIBCO™; Thermo Fisher Scientific). The cell culture was incubated at 37°C in a humidified atmosphere with 5% CO_2 and 95% air. The medium was changed twice per week. Twenty-four hours before infection 3×10^5 cells were multi-well plated on MEM medium, supplemented with 10% FBS without penicillin/streptomycin and washed twice with 500 µl MEM per well, before the infection step. A single 24-well plate was used for the cell culture method using osmotic lysis, while a single 6-well plate was used for cytofluorimetric analysis. All experiments were performed in triplicate.

2.3 | Evaluation of the frequency of internalization and intracellular persistence in the cell culture model using MG-63 osmotic lysis

The internalization frequency was evaluated in a cell culture model of infection in MG-63 osteoblasts at a multiplicity of infection (MOI) of 100:1, as previously reported (Campoccia et al., 2018). Moreover, to assess the final MOI, we previously tested MG-63 infection with ATCC12598 at 12, 50, 100, and 200 MOI, observing that with 12 and 50 MOI the ability to internalize in nonspecialized cells such as osteoblasts for *S. aureus* was very low, instead, with 200 MOI, MG-63 cultured cells showed phenomena of cytotoxicity.

Bacterial isolates were grown in Brain Heart Infusion broth (BHI; cat. No. CM1135; Oxoid Limited, Thermo Fisher Scientific Inc) at 37°C overnight. The bacterial concentration was evaluated by optical density (OD) at 600 nm. Bacterial suspensions were prepared using MEM supplemented with 10% FBS. MG-63 cultures were infected for 2 and 24 hr in antibiotic-free conditions; extracellular bacterial lysis was carried out for 1 hr at 37°C with 100 mg/ml lysostaphin (cat. No. L7386-15MG; Sigma-Aldrich, Merck KGaA; Figure A1). In addition, before and after lysostaphin treatment, the infected cell cultures were washed with PBS, and the culture medium was changed before the 24-hr incubation.

Estimation of intracellular bacteria was determined 3 hr p.i. to assess the bacterial internalization processes and 24 hr p.i. to assess persistence, by osmotic MG-63 cell lysis, serial dilution plating of the lysate on blood agar plates, incubation at 37°C overnight and CFU/ml counting. The proportion of internalized bacteria/MG-63 cells was calculated considering the MOI, the number of MG-63 cells, and the number of CFUs counted after cell lysis.

2.4 | Evaluation of the bacterial intracellular persistence frequency by imaging cytofluorimetric analysis

Infected cells, prepared as previously described at an MOI of 100:1, were first washed with 1× phosphate-buffered saline (PBS; cat. No. P5493; Sigma-Aldrich, Merck), followed by an incubation step of 3–5 min at 37°C with 0.05% trypsin-EDTA solution (cat. No. T4049; Sigma-Aldrich, Merck), and the cellular suspension was reversibly permeabilized with saponin 0.1% (cat. No. 55,255; Sigma-Aldrich, Merck) in PBS. Saponin interacts with membrane cholesterol, selectively removing it and leaving holes in the membrane. This transient permeabilization does not require cell fixing. After 15 min in saponin, the bacterial cells were labeled with 0.08 µg/ml BODIPY™ FL vancomycin (VBFL; cat. No. V34850; Invitrogen™), the membrane-impermeable green-fluorochrome vancomycin analogue that specifically binds the cell-wall peptidoglycan of Gram-positive bacteria and does not penetrate intact cells. The suspensions were then washed three times with PBS to remove the transient permeabilization and checked under the microscope to be sure that the cells had maintained their cell integrity. The labeled cellular suspension was analyzed by a FlowSight® Imaging Flow Cytometer (Amnis® FlowSight® Millipore, Merck), which quantitatively detects brightfield, darkfield, and fluorescent images with high sensitivity. This instrument acquires up to 12 images simultaneously of each cell or object including brightfield, scatter, and multiple fluorescent images at rates of up to 5,000 objects per second with high photonic sensitivity. Detailed analysis of intensity, location, and colocation of probes is achieved by IDEAS® (Image Data Exploration and Analysis Software), which offers powerful tools for statistically robust analysis of images, as well as standard flow cytometry graphing tools and statistics for hundreds of morphological features in addition to intensity. Acquisition analysis was driven by the powerful INSPIRE® and IDEAS® packages, using the main function of the INSPIRE® program during the acquisition and the IDEAS® Spot Counting analysis during results generation (Amnis, EMD Millipore).

The spots recovered in cytofluorometry imaging (total spots and full cells) were examined in a representative sample of 10,000 events, and we then theoretically normalized the result on a sample of plated cells (300,000 cells/well) and compared the total spots recovered with the whole theoretically internalized sample.

2.5 | Statistical model

Statistical analysis and the relative graphs were made using GraphPad Prism 5 (GraphPad Software Inc.). Statistical significance was assessed using Student's *t* test, both for cell culture methods and cytofluorimetric analyses. The significance threshold was set at p-value ≤ .05 (significant), p-value ≤ .01 (highly significant), and p-value ≤ .001 (extremely significant). In the cell culture assays, the colonies and the spots were counted and the data were plotted and represented as the mean ± standard deviation (*SD*) of the percentage of recovered internalized bacteria with respect to inoculated bacteria versus ATCC12598, obtained in at least two independent experiments performed in triplicate. In the flow cytometric assays, the number of single-cell events analyzed was never less than 9,980 cells out of 10,000 events at the outset.

3 | RESULTS

3.1 | Evaluation of the invasion of different MRSA genetic backgrounds in MG-63 human osteoblasts in the cell culture model

The invasiveness of different MRSA genetic backgrounds was evaluated by the cell culture infection model, using 15 invasive HA-MRSA strains belonging to the five different epidemic clones included in the study (ST239-SCC*mec*III, ST5-SCC*mec*II, ST8-SCC*mec*IV, ST228-SCC*mec*I, and ST22-SCC*mec*IVh, 3 strains for each clone) at 3 hr postinfection (p.i.). The rates of infection (CFU/infected MG-63) and ±*SD* recovered at 3 hr were **ATCC12598-ST30** $3.2 \times 10^6 \pm 3.7 \times 10^5$; **ST239-SCC*mec*III** $2.7 \times 10^6 \pm 2.8 \times 10^4$; **ST5-SCC*mec*II** $3.3 \times 10^6 \pm 5.8 \times 10^5$; **ST8-SCC*mec*IV** $2.4 \times 10^6 \pm 1.4 \times 10^5$; **ST228-SCC*mec*I** $2.8 \times 10^6 \pm 6.3 \times 10^5$; and **ST22-SCC*mec*IVh** $4.3 \times 10^6 \pm 6.8 \times 10^5$.

Three hours after the infection process, no substantial differences in the number of intracellular bacteria were observed, indicating that all analyzed strains had an internalization rate similar to one of the invasive strain ATCC12598 (Figure A2 and Table A2).

3.2 | Evaluation of the bacterial intracellular persistence frequency by imaging flow cytometric analysis—IFC

3.2.1 | Construction of the analysis template on ATCC12598

The frequencies of intracellular bacterial cells within MG-63 osteoblasts were evaluated after selective VBFL-bacterial labeling by the novel imaging flow cytometric approach using the new generation Amnis® FlowSight® Imaging Flow Cytometer.

We acquired 10,000 events for each sample and as quality control, the stained and not stained bacterial suspension to exclude autofluorescence; a negative control of infected, but not permeabilized cells, was also acquired to guarantee the exclusively intracellular localization of green spots. For each experiment, a sample of unmarked cells was acquired to exclude cellular autofluorescence or false-negative results.

The acquisition analysis was driven by INSPIRE® and IDEAS® packages. The size of every single event was established during the acquisition phase employing the scatter plot set utilizing the diameter as a parameter. This portion was referred to as a single-cell event. This first filter step was necessary to eliminate debris and cell aggregates. The 488 nm and 642 nm lasers were set to an intensity power of 30 mW for all experiments. Extracellular bacteria were efficiently disrupted by lysostaphin treatment, confirmed by the absence of fluorescence outside the MG-63 cells, in all the experiments conducted for all the samples included in the study (Figure 1).

Using IDEAS, population statistics and imaging were completely integrated; all results obtained were subdivided into two consequential steps: (a) The first analysis was performed on scatter plots using the Size Scatter in order to separate cells by size and fluorescence intensity, obtaining two large groups: labeled and unlabeled cells. On these two groups, the percentage of internalized bacteria were calculated; and (b) the second analysis was performed on a labeled cell subgroup, using the "spot counting" tool, that sets the fluorescence channel and acquires at least 20 individual events within the high and low spot categories. Evaluation of internalized bacteria by spot counting, according to the subcategories, the software identifies "N" subgroups divided by an increasing number of spots, and each subgroup was analyzed for mean fluorescence intensity (Figure 2).

3.2.2 | Analysis of the sample

Figure 3a shows the percentage of full versus empty MG-63 cells, with respect to the control strain. ATCC12598 persisted inside 51% of MG-63 at 24 hr p.i., and the same ability to persist was found in clones ST239 (47.82%) and ST22 (50.55%). The other clones analyzed were less able to persist inside MG-63, and in particular, ST5 26.59% (p = .038), ST228 20.25% (p = .0120), and ST8 19.52% (p = .0054; Table A3). Detailed data for every single strain included in the sample are reported in Figure A3 and Table A4.

These results of the internalization described above derive from Figure 3b in which we defined clones with 0 spots, 1 to 5, and over 6 spots. For the first category, 0 spots inside MG-63 cells (empty cells), the sample can be divided into two major groups, the first group included strains belonging to ST5, ST228, and ST8 and showed a percentage of empty cells ranging from 78.8% to 80% (in particular, ST5: 78.80 ± 2.46%; ST8: 79.80 ± 2.46; ST228: 80 ± 7.65%); and the second group included strains belonging to ST239, ST22, and ATCC12598 and showed about 51.5% of empty cells (in particular, ST239: 52.17 ± 7.65; ST22: 51.11 ± 5.76; ATCC12598: 51.92 ± 1.15). For the second category, 1 to 5 spots inside MG-63 cells, we found the same two groups, the first one (ST5, ST228, and ST8) showed a percentage of about 19.5% cells (in particular, ST5: 19.87 ± 2.05%; ST8: 19.49 ± 3.76; ST228: 19.35 ± 7.42%) and the second one showed a percentage ranging from 41.9% to 45% (in particular, ST239: 42.33 ± 3.4; ST22: 45.12 ± 4.16; ATCC12598: 41.97 ± 0.36). The third category, MG-63 with more than six spots inside, were less represented: 0.64 ± 0.33% for ST228, 0.71 ± 3.76% for ST8, and 1.33 ± 2.05% for ST5. Moreover, in this case, ST22 (3.77 ± 1.6%) and ST239 (5.8 ± 2.2%) showed values similar to ATCC12598 (6.11 ± 0.78%).

3.3 | Evaluation of the intracellular persistence of different MRSA genetic backgrounds in MG-63 human osteoblasts in the cell culture model

After assessing the internalization process, the proclivity to persist inside MG-63 was examined at 24 hr p.i., as reported in Figure 4a.

Although not statistically significant, the levels of intracellular bacteria changed at 24h after the infection process; in particular, ST239 (p = .99), ST8 (p = 1), and ST22 (p = .5585) showed a greater ability to persist within MG-63 osteoblasts, with respect to ST5 (p = .169) and ST228 (p = .4881) versus the ATCC12598 invasive control strain (Table A5).

3.4 | Cell culture methods versus imaging flow cytometric analysis

The rate of persistence at 24 hr was evaluated comparing the data obtained with the conventional cell culture method and data obtained with IFC and was carried out considering the number of intracellular spots per bacteria cell, as shown in Figure 4b, for each MRSA genetic background. Statistical analysis was conducted versus ATCC12598, and the percentage of internalization ± *SD*, p-values, and 95% confidence intervals are reported in Table A6.

Comparing the data set obtained with the two techniques, the rate of persistence of clones of ST239 and ST22 in MG-63 cells was

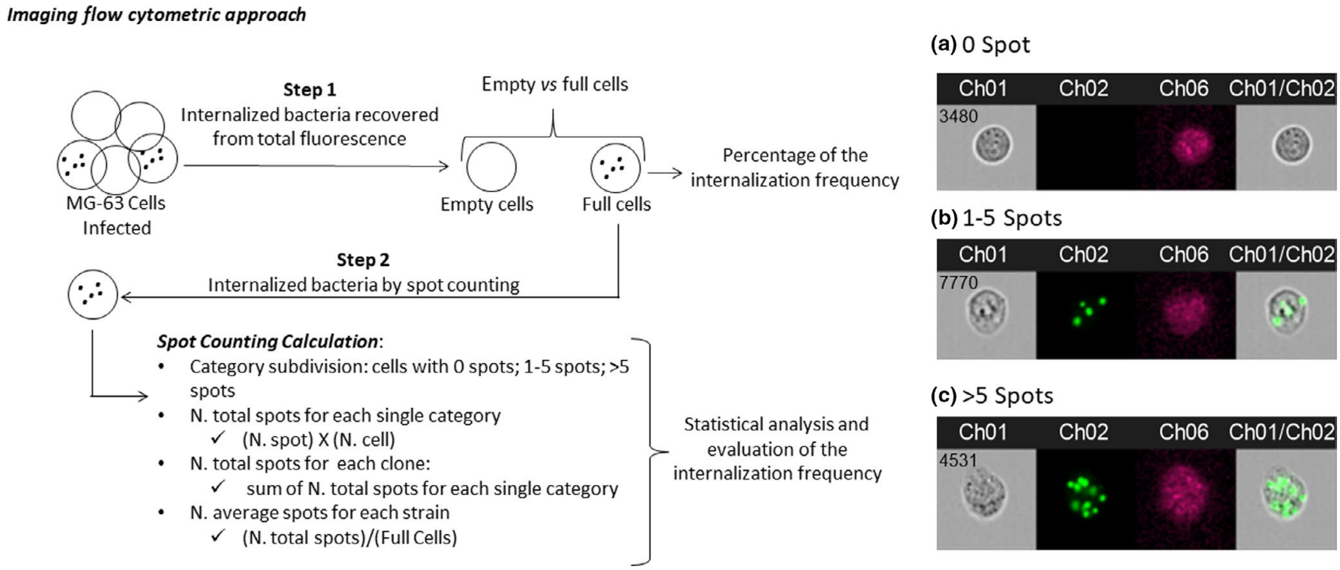

FIGURE 1 Images obtained by FlowSight® Imaging Flow Cytometer (Amnis® FlowSight® Millipore, Merck KgaA, Darmstadt, Germany), acquiring 10,000 events per sample: (a) MG-63, without spots inside the cell; (b) a single MG-63 cell with four spots inside (each spot was considered as a single bacterial cell); and (c) a single MG-63 cell with >5 spots. CH1 brightfield; CH2 band nM 505–560; CH6 Side Scatter (SSC) 785 nM; CH1/CH2 merge brightfield and 505–560 nM band

similar to that of ATCC12598; clones ST5 and ST228 were less able to persist. The only exception was clone ST8 that showed a result comparable to ATCC12598 by the cell culture method; however, this result was not confirmed by IFC.

The overall trend in all clones of the two techniques was the same; moreover, the IFC method was more sensitive as demonstrated by the *SD* values that were lower with respect to the conventional culture method.

4 | DISCUSSION AND CONCLUSIONS

Staphylococcus aureus is considered an extracellular pathogen; moreover, strains belonging to different genetic backgrounds have been known to develop an aptitude to invade and survive in phagocytic and nonphagocytic cells, and this ability can play a significant role in related diseases. Host cell invasion contributes to protecting *S. aureus* from antibiotics and the immune response and establishes a latent reservoir of bacteria that can be responsible, in particular in osteomyelitis, for the pathogenesis of this chronic and recurrent infection (Tuchscherr et al., 2011).

Staphylococcus aureus/host cell interaction is strongly conditioned by both host cell type and *S. aureus* isolate; in fact, the ability to internalize and survive in osteoblasts exhibits strain-dependent differences (Strobel et al., 2016).

In our study, different clinical MRSA strains, from invasive infections and belonging to the main worldwide HA-MRSA genetic backgrounds, were compared for their persistence ability. Our results highlighted the heterogeneity of the different clones to persist during cell infection.

The results obtained by the cell culture method demonstrated that initially (3 hr p.i.) all clones were internalized in MG-63 human osteoblasts, supporting the fact that a variety of genetic backgrounds are capable of invading host cells, but were able to differentially resist over 24 hr p.i. as demonstrated by the variable slight increase or decrease in CFU recovery; these results also suggest that osteoblasts could represent intracellular persistence niches in which *S. aureus* strains persist intracellularly and possibly replicate for a longer infection time. Our observation was supported by a previous study in which the ability of *S. aureus* to survive intracellularly for up to 7 days in osteoblasts was demonstrated (Hamza & Li, 2014).

Using the cell culture assay, we found a wide standard deviation among the different experiments for the same isolates, resulting from a large number of factors that can influence this experiment. Moreover, comparing the internalization rate of the different clones with the standard strain, no statistical significance in the ability to internalize and survive within osteoblasts was found.

The data from routine cell culture assays were improved with those obtained by the more sensitive and reliable IFC method that, together with specialized analytic software, combines the statistical power and fluorescence sensitivity of standard flow cytometry with the spatial resolution and quantitative morphology of digital microscopy, to accurately address cell counting and internalization scoring in intracellular infections (Haridas, Ranjbar, Vorobjev, Goldfeld, & Barteneva, 2017).

Fully integrated IFC and statistical analyses, with the same conditions of internalization (24 hr), allowed us to better standardize the experiments: This method was more sensitive, allowing the acquisition of a very high number of events, and was reproducible for every single sample. Our results indicated that, despite the bacterial invasion rates reflected in the trend of the cell culture data, IFC assays detected important differences that would otherwise have been undetectable.

All isolates belonging to ST5-II, ST8-IV, and ST228-I showed a statistically significant lower aptitude to intracellularly subsist

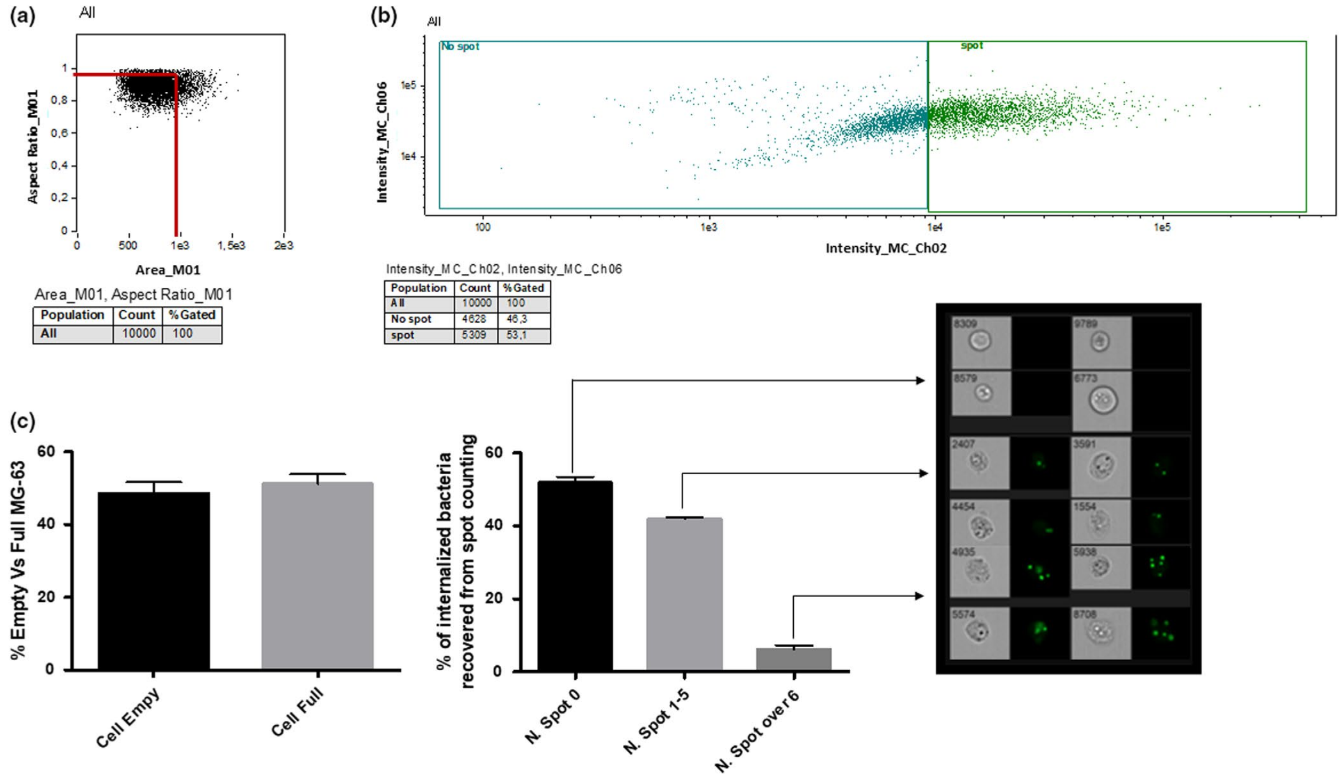

FIGURE 2 The layout used for the analysis of internalized *S. aureus* during acquisition using IFC. The layout was created for the analysis of ATCC12598 after 24 hr postinternalization in MG-63 and then applied to every single analysis for all internalization events: (a) Elimination of all events that had a noncircular shape (surface tension is responsible for the shape of liquid droplets. Although easily deformed, droplets of water tend to be pulled into a spherical shape by the cohesive forces of the surface layer. The spherical shape minimizes the necessary "wall tension" of the surface layer according to La Place's law. The cortical tension pulls the cell into a spherical shape, similar to surface tension pulling a water drop into a sphere), identifiable by the ratio between the area and the diameter, the ideal ratio of a spherical cell between width and length is 1, the graph identifies most of the events considered as "single cells" around this value. This step allowed us to acquire 10,000 events representing individual cells, eliminating debris and aggregates that would have distorted the subsequent analysis; (b) Comparison of the fluorescence intensity of the channel (in this example Ch02) corresponding to the labeled cells versus size scatter signal (Ch06). In this step, we have the creation of a cellular cloud characterized by size-shape and fluorescence quantity that divided the total amount of cells into two large groups that only differ in the amount of fluorescence. This raw analysis step precedes the more precise spot counting step; (c) Final analysis using IDEAS software that was able (after setting parameters such as Spot Low cells and High Spot cells) to identify empty and full cells (shown in the first graph), and divide the event categories by the number of "fluorescent spots." For each identified category, it was possible to evaluate the amount of fluorescence and the average fluorescence. The software organized every single gallery (deriving from a category of "number of spots" of the spot counting) based on various parameters. Each gallery was evaluated for minima and maxima fluorescence intensity, evaluating the relative accuracy of the number of spots corresponding to the category assigned by the Spot Counting

(demonstrated by both the total number of spots and the number of infected cells). All ST239-III and ST22-IVh isolates had intracellular frequencies equal to or greater than those of the reference ATCC12598 strain, suggesting their possible role as invasive and persistent clones responsible for chronic and recurrent infections.

Statistically relevant results obtained by imaging flow cytometry assays allowed us to understand that the intracellular rates did not depend on the number of bacterial cells that manage to enter/replicate inside a single MG-63 osteoblast, but on the total number of cells that were infected. The ability to internalize and persist inside osteoblasts seems, therefore, not only related to the clone but to other factors that deserve to be investigated.

Furthermore, our observations have been supported by the increase, in the last ten years, of strains belonging to ST239 and ST22 associated with bacteremia and PJIs (Coombs, Daley, Lee, Pang, 2019; Jain, Chowdhury, Datta, Chowdhury, & Mukhopadhyay, 2019; Peng et al., 2019) and probably associated with prophage-mediated virulence determinants (*sas*X), crucial for colonization, immune evasion, and host cell invasion (Bakthavatchalam, Triplicane Dwarakanathan, Munusamy, Jennifer, & Veeraraghavan, 2019).

This study presents some limitations that should be mentioned: whole-genome sequencing analysis, for detecting different genetic variants and gene-expression studies, and for determining whether a particular gene or set of genes is responsible for the specific internalization behavior, was not performed. The pathogenic and molecular characteristics that enhance the aptitude to internalize in, escape from, or persist within host cells undoubtedly reside in the differential expression of regulatory and virulence genes (Horn et al., 2018; Josse et al., 2015).

The current study contributes to our understanding of the differential interaction between osteoblasts and invasive MRSA strains

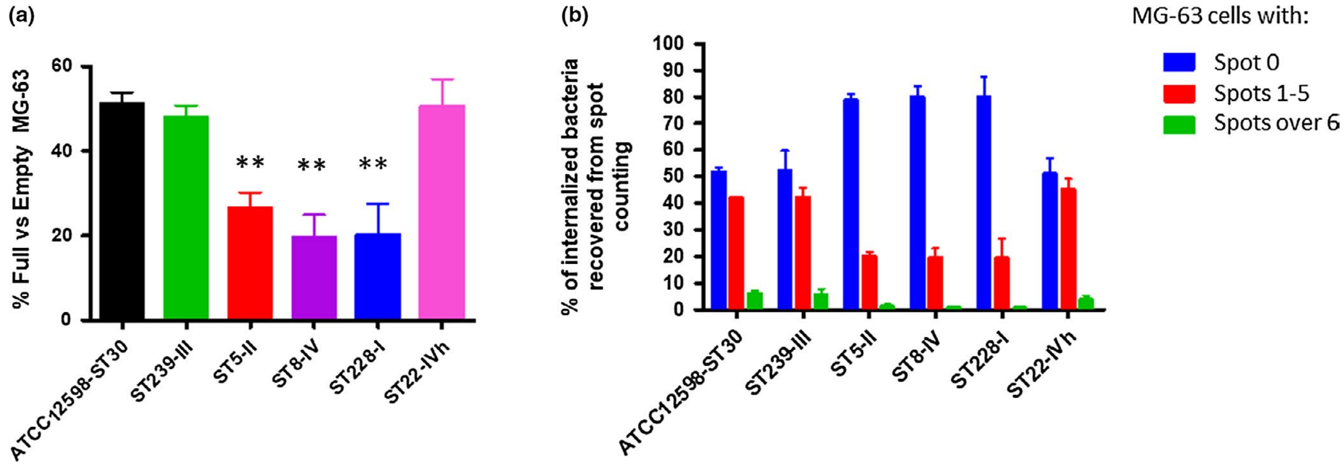

FIGURE 3 (a) Evaluation of the internalization frequency by IFC. After 24 hr p.i. at an MOI of 100:1, external and adherent bacteria were removed by lysostaphin treatment. The MG-63 cells infected with the different strains were stained with the membrane-impermeable fluorochrome VBFL and analyzed on a flow cytometer (Amnis FlowSight Millipore), acquiring 10,000 events per sample. The graph reports the percentage of spots for cell ± *SD* for each strain for three different experiments. Statistical significative *p*-value ≤ .05 *; highly significative ≤.01**; extremely significative ≤.001***. (b) Invasion rate of MRSA strains from different genetic backgrounds. After 2 hr of infection at an MOI of 100:1, external and adherent bacteria were removed by lysostaphin treatment for 1 hr. The infected MG-63 cells were lysed at 24 hr postinfection after a lysostaphin treatment for 1 hr. The MG-63 cells infected with the different strains were osmotically lysed, and the number of intracellular bacteria was determined by plating serial dilutions of the lysates on blood agar plates and counting the colonies grown after overnight incubation. The graph reports the mean ± *SD* for each clone for three different experiments

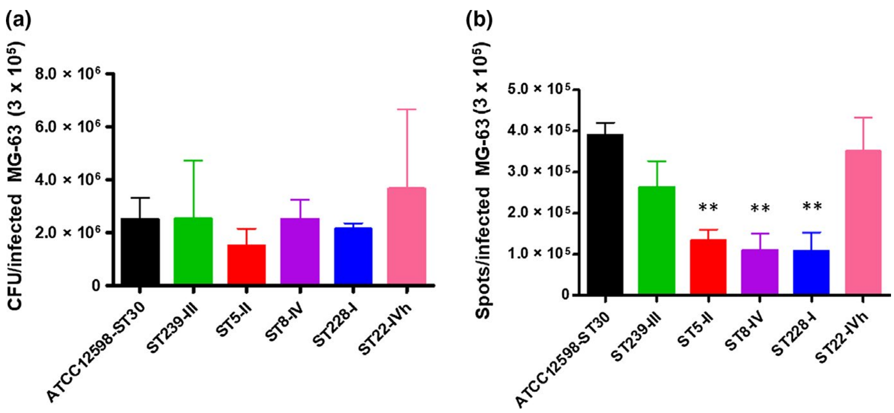

FIGURE 4 Evaluation of the persistence frequency by IFC evaluation, after 24 hr p.i. at an MOI of 100:1, external and adherent bacteria were removed by lysostaphin treatment. The MG-63 cells infected with the different strains were stained with the membrane-impermeable fluorochrome VBFL and analyzed on a flow cytometer (Amnis FlowSight Millipore), acquiring 10,000 events per sample. (a) The graph shows the distribution of spots corresponding to the category assigned by the Spot Counting, for each clone. (b) The graph shows the percentage of full versus empty cells, recovered from spot counting. The graph reports the percentage of spots for cell ± *SD* for each strain for three different experiments. Statistical significative *p*-value ≤ .05*; highly significative ≤ .01**; extremely significative ≤ .001***

belonging to different genetic backgrounds. By means of an imaging flow cytometry-based approach, we demonstrated that internalization is a pathophysiological pathway of some MRSA depending on the total number of cells infected and not on the bacterial cells that enter each osteoblast. Furthermore, even if our strains were not homogeneous in terms of genetic backgrounds and virulence factors, ST22-IVh and ST239-III showed higher intracellular persistence in host cells, making them more prone to developing chronic and recurrent infections. We believe that our study provides additional information useful to predict the proclivity of some staphylococcal clones associated with recurrent and chronic infections, to invade, internalize, and persist within human cells, with respect to others.

ACKNOWLEDGMENTS

Some of the results of this study were presented at the 29th ECCMID (O0927) and the 44th Italian Society of Microbiology (SIM) congress (P127). We would like to thank professor V. Cardile and A. Graziano, and the BRIT laboratory at the University of Catania (Italy) for valuable technical assistance and laboratories and in particular to S. Grimaldi. The manuscript was partially supported by a research grant project number PRIN2017SFBFER form Minister of Research (MIUR), Italy; a research grant for a private company; a research grant entitled "Identification of cancer driver genes for novel diagnostics and therapeutic strategies—Piano per la ricerca 2016-2018—Linea di intervento 2—University of Catania, Dept. of Biomedical and Biotechnological Sciences." We also wish to thank the Scientific Bureau of the University of Catania for language support.

CONFLICT OF INTERESTS

None declared.

AUTHOR CONTRIBUTIONS

Dafne Bongiorno equally contributed to conceptualization, data curation, formal analysis, methodology, validation, writing–original draft, and writing–review and editing; Nicolò Musso equally contributed to conceptualization, data curation, formal analysis, methodology, software, validation, and writing–original draft; Lorenzo Lazzaro equally contributed to methodology and made supporting role in validation; Gino Mongelli equally contributed to investigation and methodology, and made supporting role in validation; Stefania Stefani equally contributed to funding acquisition, resources, supervision, validation, and writing–review and editing; Floriana Campanile equally contributed to conceptualization, funding acquisition, project administration, supervision, writing–original draft, and writing–review and editing.

ETHICS STATEMENT

None required.

DATA AVAILABILITY STATEMENT

All data are provided in full in the results section of this paper and in the Appendices 1 and 2.

ORCID

Dafne Bongiorno https://orcid.org/0000-0002-8672-0484
Nicolò Musso https://orcid.org/0000-0003-2451-1158
Gino Mongelli https://orcid.org/0000-0003-0976-2936
Stefania Stefani https://orcid.org/0000-0003-1594-7427
Floriana Campanile https://orcid.org/0000-0002-8405-5425

REFERENCES

Bakthavatchalam, Y. D., Triplicane Dwarakanathan, H., Munusamy, E., Jennifer, L., & Veeraraghavan, B. (2019). A distinct geographic variant of *sasX* in methicillin-resistant *Staphylococcus aureus* ST239 and ST368 lineage from South India. *Microbial Drug Resistance*, *25*, 413–420.

Bongiorno, D., Mongelli, G., Stefani, S., & Campanile, F. (2018). Burden of rifampicin- and methicillin-resistant *Staphylococcus aureus* in Italy. *Microbial Drug Resistance*, *24*, 732–738.

Campanile, F., Bongiorno, D., Perez, M., Mongelli, G., Sessa, L., Benvenuto, S., … Stefani, S. (2015). Epidemiology of *Staphylococcus aureus* in Italy: First nationwide survey. *Journal of Global Antimicrobial Resistance*, *3*, 247–254.

Campoccia, D., Montanaro, L., Ravaioli, S., Cangini, I., Testoni, F., Visai, L., & Arciola, C. R. (2018). New parameters to quantitatively express the invasiveness of bacterial strains from implant-related orthopaedic infections into osteoblast cells. *Materials*, *11*, 550. https://doi.org/10.3390/ma11040550

Coombs, G. W., Daley, D. A., Lee, Y. T., & Pang, S. (2019). Australian Group on Antimicrobial Resistance (AGAR) Australian *Staphylococcus aureus* Sepsis Outcome Programme (ASSOP) Annual Report 2017. *Communicable Diseases Intelligence*, *16*, 43. https://doi.org/10.33321/cdi.2019.43.43

Garzoni, C., & Kelley, W. L. (2009). *Staphylococcus aureus*: New evidence for intracellular persistence. *Trends in Microbiology*, *17*, 59–65. https://doi.org/10.1016/j.tim.2008.11.005

Gould, I. M., Gauda, R., Esposito, S., Gudiol, F., Mazzei, T., & Garau, J. (2011). Management of serious methicillin-resistant *Staphylococcus aureus* infection: What are the limits? *International Journal of Antimicrobial Agents*, *37*, 202–209.

Hamza, T., & Li, B. (2014). Differential responses of osteoblasts and macrophages upon *Staphylococcus aureus* infection. *BMC Microbiology*, *14*, 207. https://doi.org/10.1186/s12866-014-0207-5

Haridas, V., Ranjbar, S., Vorobjev, I. A., Goldfeld, A. E., & Barteneva, N. S. (2017). Imaging flow cytometry analysis of intracellular pathogens. *Methods*, *112*, 91–104. https://doi.org/10.1016/j.ymeth.2016.09.007

Horn, J., Stelzner, K., Rudel, T., & Fraunholz, M. (2018). Inside job: *Staphylococcus aureus* host-pathogen interactions. *International Journal of Medical Microbiology*, *308*, 607–624. https://doi.org/10.1016/j.ijmm.2017.11.009

Jain, S., Chowdhury, R., Datta, M., Chowdhury, G., & Mukhopadhyay, A. K. (2019). Characterization of the clonal profile of methicillin resistant *Staphylococcus aureus* isolated from patients with early post-operative orthopaedic implant-based infections. *Annals of Clinical Microbiology and Antimicrobials*, *18*, 8.

Jevon, M., Guo, C., Ma, B., Mordan, N., Nair, S. P., Harris, M., … Meghji, S. (1999). Mechanisms of internalization of *Staphylococcus aureus* by cultured human osteoblasts. *Infection and Immunity*, *67*, 2677–2681. https://doi.org/10.1128/IAI.67.5.2677-2681.1999

Josse, J., Guillaume, C., Bour, C., Lemaire, F., Mongaret, C., Draux, F., … Gangloff, S. C. (2016). Impact of the maturation of human primary bone-forming cells on their behaviour in acute or persistent *Staphylococcus aureus* infection models. *Frontiers in Cellular and Infection Microbiology*, *6*, 64.

Josse, J., Velard, F., & Gangloff, S. C. (2015). *Staphylococcus aureus vs* Osteoblast: Relationship and consequences in osteomyelitis. *Frontiers in Cellular and Infection Microbiology*, *5*, 85. https://doi.org/10.3389/fcimb.2015.00085

McPherson, J. C., Runner, R. R., Shapiro, B., Walsh, D. S., Stephens-DeValle, J., & Buxton, T. B. (2008). An acute osteomyelitis model in traumatized rat tibiae involving sand as a foreign body, thermal injury, and microbial contamination. *Comparative Medicine*, *58*, 369–374.

Moore, A. J., Whitehouse, M. R., Gooberman-Hill, R., Heddington, J., Beswick, A. D., Blom, A. W., & Peters, T. J. (2017). A UK national survey of care pathways and support offered to patients receiving revision surgery for prosthetic joint infection in the highest volume NHS orthopaedic centres. *Musculoskeletal Care*, *15*, 379–385. https://doi.org/10.1002/msc.1186

Peng, K. T., Huang, T. Y., Chiang, Y. C., Hsu, Y. Y., Chuang, F. Y., Lee, C. W., & Chang, P. J. (2019). Comparison of methicillin-resistant *Staphylococcus aureus* Isolates from cellulitis and from osteomyelitis in a Taiwan Hospital, 2016–2018. *Journal of Clinical Medicine*, *8*, 816.

Purrello, S. M., Garau, J., Giamarellos, E., Mazzei, T., Pea, F., Soriano, A., & Stefani, S. (2016). Methicillin-resistant *Staphylococcus aureus* infections: A review of the currently available treatment options. *Journal of Global Antimicrobial Resistance*, *7*, 178–186.

Sinha, B., & Fraunholz, M. (2010). *Staphylococcus aureus* host-cell invasion and post-invasion events. *International Journal of Medical Microbiology*, *300*, 170–175. https://doi.org/10.1016/j.ijmm.2009.08.019

Stefani, S., Chung, D. R., Lindsay, J. A., Friedrich, A. W., Kearns, A. M., Westh, H., & Mackenzie, F. M. (2012). Meticillin-resistant *Staphylococcus aureus* (MRSA): Global epidemiology and harmonisation of typing methods. *International Journal of Antimicrobial Agents*, *39*, 273–282. https://doi.org/10.1016/j.ijantimicag.2011.09.030

Strobel, M., Pförtner, H., Tuchscherr, L., Völker, U., Schmidt, F., Kramko, N., … Niemann, S. (2016). Post-invasion events after infection with *Staphylococcus aureus* are strongly dependent on both the host-cell type and the infecting *S. aureus*strain. *Clinical Microbiology & Infection*, *22*, 799–809.

Trouillet, S., Rasigade, J. P., Lhoste, Y., Ferry, T., Vandenesch, F., Etienne, J., & Laurent, F. (2011). A novel Flow Cytometry-based assay for the quantification of *Staphylococcus aureus* adhesion to and invasion of eukaryotic cells. *Journal of Microbiological Methods*, *86*, 145–149. https://doi.org/10.1016/j.mimet.2011.04.012

Tuchscherr, L., & Löffler, B. (2016). *Staphylococcus aureus* dynamically adapts global regulators and virulence factor expression in the course from acute to chronic infection. *Current Genetics*, *62*, 15–17.

Tuchscherr, L., Medina, E., Hussain, M., Völker, W., Heitmann, V., Niemann, S., … Löffler, B. (2011). *Staphylococcus aureus* phenotype switching: An effective bacterial strategy to escape host immune response and establish a chronic infection. *EMBO Molecular Medicine*, *3*, 129–141.

Valour, F., Trouillet-Assant, S., Rasigade, J. P., Lustig, S., Chanard, E., Meugnier, H., … Lyon BJI Study Group (2013). *Staphylococcus epidermidis* in orthopedic device infections: The role of bacterial internalization in human osteoblasts and biofilm formation. *PLoS ONE*, *28*(8), e67240. https://doi.org/10.1371/journal.pone.0067240

Wright, K. M., & Friedland, J. S. (2004). Regulation of chemokine gene expression and secretion in *Staphylococcus aureus*-infected osteoblasts. *Microbes and Infection*, *6*, 844–852.

How to cite this article: Bongiorno D, Musso N, Lazzaro LM, Mongelli G, Stefani S, Campanile F. Detection of methicillin-resistant *Staphylococcus aureus* persistence in osteoblasts using imaging flow cytometry. *MicrobiologyOpen*. 2020;9:e1017. https://doi.org/10.1002/mbo3.1017

APPENDIX 1

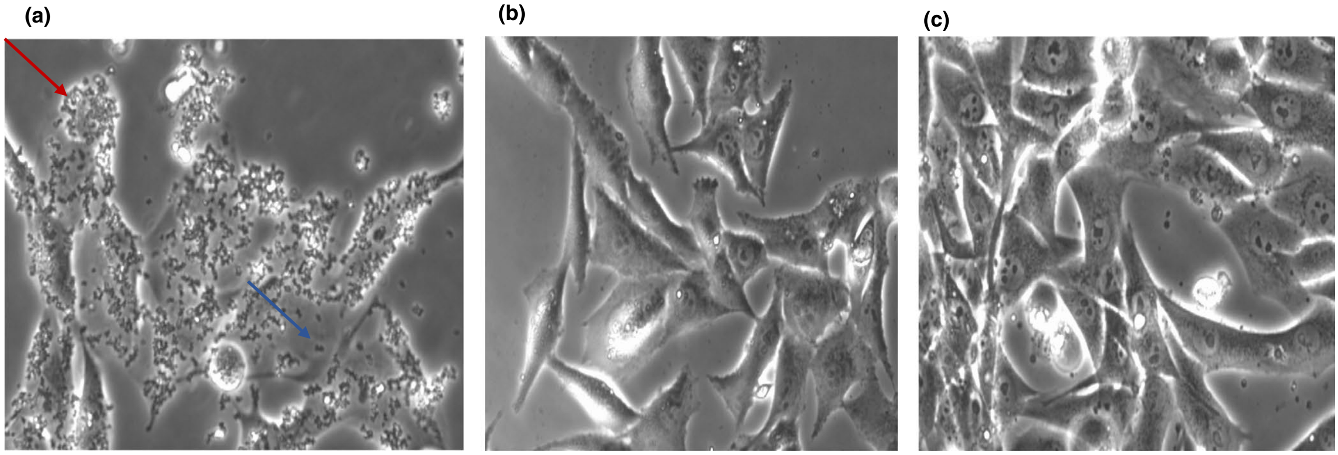

FIGURE A1 Image obtained with Leica DMI 4,000 20× (a, b and c). (a) MG-63 after 1h of infection with 7SA-ST8-SCC*mec*IV, bacterial cells were present all around the MG-63 cells (red arrow) and in the cell culture space between MG-63 cells (blue arrow); (b) after 2 hr of infection and 1 hr of lysostaphin treatment, there were no bacteria in cell culture spaces between MG-63 cells, and (c) the MG-63 cell culture after 24 hr of infection

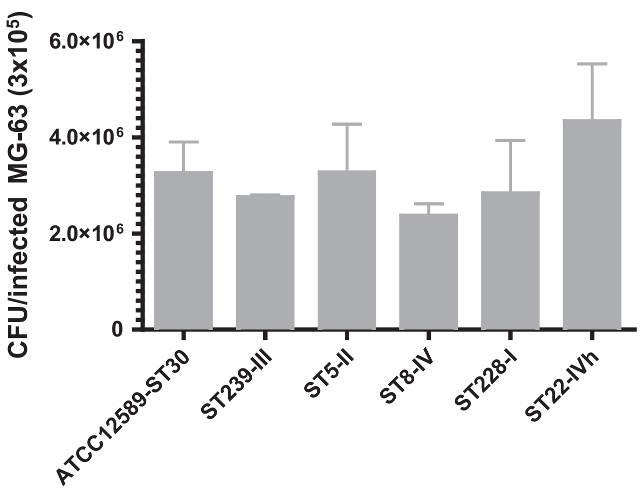

FIGURE A2 Invasion rate of MRSA strains from different genetic backgrounds. After 2 hr of infection at an MOI of 100:1, external and adherent bacteria were removed by lysostaphin treatment for 1 hr. The MG-63 cells infected with the different strains were osmotically lysed, and the number of intracellular bacteria was determined by plating serial dilutions of the lysates on blood agar plates and counting the colonies grown after overnight incubation at 37°C. The graph reports the mean ± *SD* for each clone for two different experiments

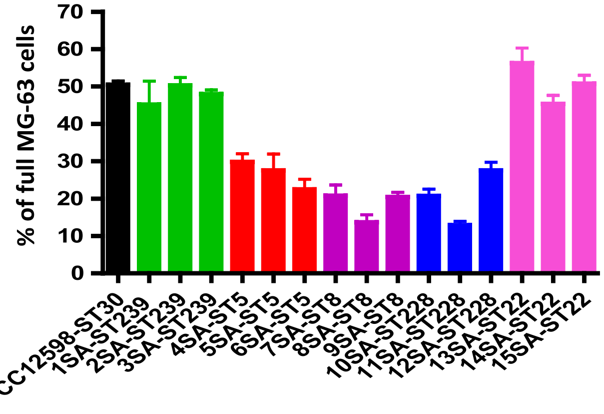

FIGURE A3 Evaluation of the internalization frequency by IFC. At 24 hr p.i. at an MOI of 100:1, external and adherent bacteria were removed by lysostaphin treatment. The MG-63 cells infected with the different strains were stained with the membrane-impermeable fluorochrome VBFL and analyzed on a flow cytometer (Amnis FlowSight Millipore), acquiring 10,000 events per sample. The graph reports the average amount of spots per cell ± *SD* for each strain for three different experiments

APPENDIX 2

TABLE A1 The table reports the phenotypical and molecular characteristics of the sample included in the study

LAB CODE	ST-SCC*mec*-Spa type	Source	FOX	CN	DA	E	CIP	TE	SXT	K	RD	BPR	DAL	CPT	LNZ	DPT	TGC	FU	VA	TC	GRD
1SA	239-III- t030	Wound	R	R	R	R	S	R	S	R	>32	2	0.125	2	2	1	0.25	>256	0.5	0.25	VSSA
2SA	241-III-t037	Wound	R	R	Ri	R	R	R	R	R	2	2	0.125	2	2	0.5	0.25	>256	1	2	VSSA
3SA	239-III-t037	Blood	R	R	Ri	R	R	R	R	R	2	1	0.25	2	2	1	0.25	>256	1	0.5	VSSA
4SA	5-II-t002	Blood	R	R	Ri	R	R	R	S	S	16	4	0.125	4	4	0.5	0.5	4	1	2	VSSA
5SA	5-II-t2154	Blood	R	R	S	R	R	R	S	R	>32	2	0.012	4	32	0.5	0.5	>256	1	0.5	hVISA
6SA	5-II-t002	CVC	R	S	R	R	R	S	S	R	0.008	4	0.125	2	1	1	0.125	0.064	1	0.5	hVISA
7SA	8-IV-t008	Hip fistula	R	R	R	R	R	R	S	R	>32	2	0.125	2	4	1	0.125	0.064	2	2	hVISA
8SA	8-IVc-t008	Bronchial	R	S	S	S	R	S	S	S	0.008	2	0.125	2	0.5	0.5	0.125	0.125	1	1	VSSA
9SA	8-IVc-t008	Bronchial	R	R	S	R	R	S	S	R	0.016	1	0.064	1	0.5	0.5	0.125	0.125	2	0.5	hVISA
10SA	228-I-t041	Blood	R	R	R	R	R	S	S	R	>32	2	0.125	1	8	1	0.125	0.125	1	1	VSSA
11SA	228-I-t041	Knee biopsy	R	R	R	R	R	I	S	R	2	2	0.064	4	2	0.5	0.125	0.064	2	1	hVISA
12SA	228-I-t001	CVC	R	R	Ri	R	R	S	S	R	0.016	2	0.064	2	0.5	0.5	0.125	0.125	1	2	VSSA
13SA	22-IVh-t032	Blood	R	R	S	S	R	R	S	R	>32	0.5	0.125	1	0.5	0.5	0.06	0.125	1	0.25	VSSA
14SA	22-IVh-t032	Blood	R	S	Ri	R	R	S	S	S	0.008	1	0.064	1	1	1	0.125	0.064	0.5	0.25	VSSA
15SA	22-IVh-t902	Blood	R	S	Ri	R	S	R	S	S	>32	1	0.125	0.5	2	2	0.064	0.125	1	0.25	VSSA

Abbreviations: FOX, cefoxitin; CN, gentamicin; DA, clindamycin; E, erythromycin; CIP, ciprofloxacin; TE, tetracycline; SXT, trimethoprim/sulfamethoxazole; K, kanamycin; RD, rifampin; BPR, ceftobiprole; DAL, dalbavancin; CPT, ceftaroline; LNZ, linezolid; DPT, daptomycin; TGC, tigecycline; FU, fusidic acid; VA, vancomycin; TC, teicoplanin; GRD, MIC test strip glycopeptide resistance detection; Ri, Inducible clindamycin resistance; clone characterization by means of: ST, Sequence Type; SCC*mec*, Staphylococcal Cassette Chromosome *mec*; *spa* type, staphylococcal protein A.

TABLE A2 The statistical analysis relative to strain invasiveness was performed by comparing the rate of infection of each strain with the rate of infection of ATCC12598 as control for cell culture method at 3 hr p.i., using *t* test, *p* value and 95% of confidence

t Test	ATCC12598-ST30	ST239-SCCmecIII	ST5-SCCmecII	ST8-SCCmecIV	ST228-SCCmecI	ST22-SCCmecIVh
Rate of Infection CFU/ infected MG-63	$3.2 \times 10^6 \pm 3.7 \times 10^5$	$2.7 \times 10^6 \pm 2.8 \times 10^4$	$3.3 \times 10^6 \pm 5.8 \times 10^5$	$2.4 \times 10^6 \pm 1.4 \times 10^5$	$2.8 \times 10^6 \pm 6.3 \times 10^5$	$4.3 \times 10^6 \pm 6.8 \times 10^5$
p value	—	.2548	.9819	.0932	.6016	.2394
95% confidence interval	—	-1.545×10^6 to 5.455×10^5	-1.904×10^6 to 1.937×10^6	-2.001×10^6 to 2.34×10^5	-2.461×10^6 to 1.627×10^6	-1.095×10^6 to 3.26×10^6

TABLE A3 The statistical analysis relative to strain invasiveness was performed by comparing the rate of infection of each strain with the rate of infection of ATCC12598 as control for cell culture method at 3 hr p.i., using *t* test, *p* value and 95% of confidence

t Test	ACTT12598-ST30	ST239-SCCmecIII	ST5-SCCmecII	ST8-SCCmecIV	ST228-SCCmecI	ST22-SCCmecIVh
% of internalization ± *SD*	51.18 ± 1.19	47.82 ± 1.68	26.59 ± 2.05	12.52 ± 3.185	20.25 ± 4.24	50.55 ± 3.71
p-Value of internalized bacteria recovered from spot counting versus ATCC12598	–	.2876	**.038***	**.0054*****	**.0120****	.9077
95% confidence interval	–	4.921 to −11.63	15.01 to −34.16	17.82 to 4.551	12.93 to 48.93	15.28 to −16.54

Note: The table reports the detailed statistical data obtained using *t* test versus ATCC12598: % of internalization, *p*-value and 95% confidence. Statistically significant *p*-value ≤.05*; highly significant ≤.01**; extremely significant ≤.001***.

The bold values are statistically significant.

TABLE A4 The statistical analysis relative to strain invasiveness was performed by comparing the rate of infection of each strain with the rate of infection of ATCC12598 as control for cell culture method at 3 hr p.i., using *t* test, *p* value and 95% of confidence

t Test	ATCC12598-ST30	1SA-ST239	2SA-ST239	3SA-ST239	4SA-ST5	5SA-ST5	6SA-ST5
% of internalization ± *SD*	50.49 ± 0.69	45.20 ± 3.58	50.33 ± 1.19	47.98 ± 0.63	29.82 ± 1.2	27.59 ± 2.5	22.49 ± 1.58
p-Value N cells versus ATCC12598	—	.3380	.9261	.0791	**.0012****	**.006****	**.0008****
95% confidence interval	—	−20.09 to −9.513	−5.320 to 4.994	−5.568 to −0.5416	−26.12 to −15.22	−33.34 to −12.46	−34.49 to −21.50

Note: The table reports the detailed statistical data obtained using *t* test versus ATCC12598: % of internalization, *p*-value and 95% of confidence. Statistically significant *p*-value ≤.05*; highly significant ≤.01**, extremely significant ≤.001***.

The bold values are statistically significant.

TABLE A5 The statistical analysis relative to strain invasiveness was performed by comparing the rate of infection of each strain with the rate of infection of ATCC12598 as control for cell culture method at 3 hr p.i., using *t* test, *p* value and 95% of confidence

t Test	ATCC12598-ST30	ST239-SCC*mec*III	ST5-SCC*mec*II
Rate of Infection CFU/infected MG-63	$1.9 \times 10^6 \pm 4.6 \times 10^5$	$2.5 \times 10^6 \pm 1.8 \times 10^5$	$1.5 \times 10^6 \pm 3.8 \times 10^5$
p Value	—	.99	.169
95% confidence interval	—	-3.774×10^5 to 3.741×10^6	-6.592×10^5 to 2.666×10^6

TABLE A6 The statistical analysis relative to strain invasiveness was performed by comparing the rate of infection of each strain with the rate of infection of ATCC12598 as control for cell culture method at 3 hr p.i., using *t* test, *p* value and 95% of confidence.

t Test	ATCC12598-ST30	ST239-SCC*mec*III	ST5-SCC*mec*II	ST8-SCC*mec*IV	ST228-SCC*mec*I	ST22-SCC*mec*IVh
Average spots/ infected MG−63	$3.9 \times 10^5 \pm 2.1 \times 10^4$	$2.6 \times 10^5 \pm 3.6 \times 10^4$	$1.3 \times 10^5 \pm 2.5 \times 10^4$	$1.1 \times 10^5 \pm 2.4 \times 10^4$	$1.08 \times 10^5 \pm 2.6 \times 10^4$	$3.5 \times 10^5 \pm 4.7 \times 10^4$
p Value	—	.084	**.002**	**.004**	**.0049**	.5762
95% confidence interval	—	-3.14×10^5 to 2.84×10^4	1.76×10^5 to 3.37×10^4	1.69×10^5 to 3.91×10^4	1.62×10^5 to 4.01×10^4	-1.61×10^5 to 2.40×10^4

Note: Statistical data versus ATCC12598, using *t* test, *p* value and 95% of confidence. Statistically significant *p*-value ≤.05*; highly significant ≤.01**, extremely significant ≤.001***.

The bold values are statistically significant.

7SA-ST8	8SA-ST8	9SA-ST8	10SA-ST228	11SA-ST228	12SA-ST228	13SA-ST22	14SA-ST22	15SA-ST22
20.78 ± 1.659	13.68 ± 1.34	20.43 ± 0.72	20.74 ± 1.04	12.89 ± 0.59	27.59 ± 1.12	56.24 ± 2.34	45.37 ± 1.31	50.70 ± 1.27
.0009**	**.0002****	**<.0001*****	**.0002**	**<.0001**	**.0009**	.1573	.0633	.8725
−36.72 to 22.70	−41.74 to −31.87	−33.44 to 29.69	−34.33 to −25.18	−40.54 to −32.56	−28.26 to −17.54	−4.005 to 15.51	−10.78 to 0.5308	−5.169 to 5.769

ST8-SCC*mec*IV	ST228-SCC*mec*I	ST22-SCC*mec*IVh
$2.5 \times 10^6 \pm 4.3 \times 10^5$	$2.1 \times 10^6 \pm 1.3 \times 10^5$	$3.6 \times 10^6 \pm 1.7 \times 10^6$
1.0	.4881	.5585
-1.763×10^6 to 1.763×10^6	-9.670×10^5 to 1.701×10^6	-6.129×10^6 to 3.84×10^6